Available online at www.sciencedirect.com
ScienceDirect
Journal of Colloid and Interface Science 319 (2008) 590–593
JOURNAL OF Colloid and Interface Science
www.elsevier.com/locate/jcis

Note

Effects of additives on the structure of rhamnolipid (biosurfactant): A small-angle neutron scattering (SANS) study

Behnaz Dahrazma [a], Catherine N. Mulligan [b,*], Mu-Ping Nieh [c]

[a] *Department of Environmental Geology Faculty of Earth Science, Shahrood University of Technology, Shahrood 316-3619995161, Iran*
[b] *Department of Building, Civil and Environmental Engineering, Concordia University, EV 6-187, 1455 de Maisonneuve Blvd. W., Montreal, PQ, H3G 1M8, Canada*
[c] *Canadian Neutron Beam Centre, Steacie Institute for Molecular Sciences, National Research Council Canada, Chalk River, ON, K0J 1J0, Canada*

Received 14 June 2007; accepted 20 November 2007

Available online 5 December 2007

Abstract

Pollution of soils and sediments by heavy metals is an environmental concern. Among the remedial techniques, soil washing is proving to be reliable. Biosurfactant rhamnolipid has shown its potential as a washing agent. In this research, small angle neutron scattering (SANS) was employed to investigate the size and morphology of rhamnolipid aggregates and micelle structure in the presence of heavy metals Cu, Zn, and Ni. The results indicate the importance of the pH of the system in the morphology of the aggregates in the rhamnolipid solution. Creation of a basic condition by addition of 1% NaOH led to the formation of large aggregates (>2000 Å) + micelles with $R_G \sim 17$ Å while in the acidic environment with 1% NaCl, large polydisperse vesicles with a radius about 550–600 Å were formed. The size of the aggregates in both acidic and basic condition is fine enough to ease the flow of the rhamnolipid solution through the porous media with the pore sizes as small as 200 nm.

Keywords: SANS; Rhamnolipids; Heavy metals; Soil remediation; Micelle structure

1. Introduction

Biosurfactants are surface active agents produced by microorganisms. The rhamnolipids used in this study, R1 and R2, are biosurfactants from the glycolipid group produced by the bacterium *Pseudomonas aeruginosa* the chemical structures of which are shown in Fig. 1 [1,2]. They are capable of effectively removing heavy metals (such as copper and zinc) from sediments [3,4] and enhancing the removal of oil grease and metal ions from contaminated soil [5–7]. This capacity opens a new horizon to study the extraction of copper from ore. Up to 53.4% of copper was extracted from a mining residue using 5% rhamnolipid [8]. Addition of 1% NaOH showed significant enhancement of the removal of copper from sediments and mining residues [9]. The changes in heavy metal removal efficiency under different conditions presumably pertain to the change in the structure of rhamnolipid [6,8,10]. It is known that a variety of morphologies of rhamnolipid exist including lamellar, vesicles and micelles [11]. The structures of rhamnolipids were previously studied using polarized optical microscopy (POM) and cryo-transmission electron microscopy (cryo-TEM) to sample the structure of rhamnolipid micelles locally upon varying electrolytes (metal ions), pH and alkanes [12,13]. Small angle neutron scattering (SANS), a complementary technique to POM and cryo-TEM, is able to provide the average global morphology of aggregates in solutions and has also been widely used in resolving the structures of surfactants, phospholipids and microemulsions with the length scale ranged from 10 to 1000 Å. In this study, the objective was to use SANS to investigate the morphology of the rhamnolipid in the absence and the presence of different additives including NaOH, KOH, NaCl, and heavy metal ions such as Cu^{2+}, Zn^{2+}, and Ni^{2+} to obtain more insight in to the structural transformations.

* Corresponding author. Fax: +1 514 848 7925.
E-mail address: mulligan@civil.concordia.ca (C.N. Mulligan).

0021-9797/$ – see front matter
doi:10.1016/j.jcis.2007.11.045

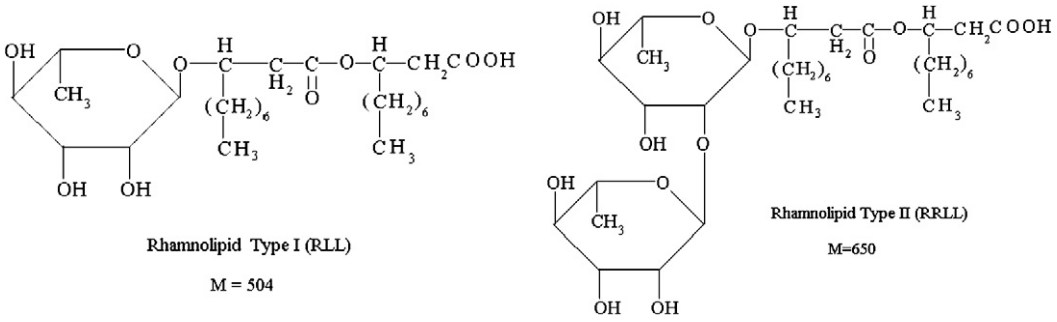

Fig. 1. Structure of rhamnolipid types I and II.

2. Materials and methods

2.1. Materials

The rhamnolipids, used in this study, were biosurfactants type I, RLL (R1), and type II, RRLL (R2), from the glycolipid group made by *Pseudomonas aeruginosa* with the trademark JBR215 from Jeneil Biosurfactant Co. JBR215 is an aqueous solution of rhamnolipid at 15% concentration. It is produced from a sterilized and centrifuged fermentation broth. The molecular formula of R1 is $C_{26}H_{48}O_9$ and that of R2 is $C_{32}H_{58}O_{13}$.

2.2. Sample preparation

According to the literature [3,4,10], working with the concentration of 2% rhamnolipid is the most practical in soil washing. The samples run at the Canadian Neutron Beam Centre (CNBC, Chalk River, ON, Canada) were prepared with and without 100 mg/L of copper, nickel and zinc individually in 2% rhamnolipid in D_2O adjusting the pH to 5 and 13. The samples for further detailed neutron scattering study at National Institute of Standards and Technology (NIST) Center for Neutron Research (NCNR, Gaithersburg, MD, USA) were prepared in the same manner including 100 mg/L of all ions (Cu^{2+}, Ni^{2+} and Zn^{2+}) in 2% rhamnolipid in D_2O. The pH of the samples using no additives (S#1), 1% NaOH (S#2), 1% KOH (S#3), and 1% NaCl (S#4), were measured at 6.5, 13.2, 13.2, and 5.5, respectively. The pH of the S#1 was adjusted using 10% HNO_3 and NaOH (1 M).

2.3. Instrument and data reduction

SANS experiments were conducted at both NIST (National Institute of Standards and Technology) Center for Neutron Research (NCNR, Gaithersburg, MD, USA) and Canadian Neutron Beam Centre (CNBC, Chalk River, ON, Canada).

2.3.1. NG3 30 m SANS instruments at NCNR

A neutron wavelength (λ) of 6 Å and three sample-to-detector distances (1, 5, and 13 m) were employed, covering a q-range of $0.003 < q < 0.3$ Å^{-1} where q is defined as $4\pi/\lambda \sin\theta/2$, where θ is the scattering angle between the incident and the scattered neutron beams. Samples were placed into demountable cells with a path length of 2 mm. The 2-D raw data were corrected for the ambient background and empty cell scattering and normalized to yield an absolute scale (cross section per unit volume) by the neutron flux on the samples [14]. The data were then circularly averaged to yield the 1-D intensity distribution, $I(q)$. The incoherent scattering was approximated from the high q intensity plateau and subtracted from the corresponding reduced data.

2.3.2. E3 neutron diffractometer at CNBC

A neutron wavelength of 2.37 Å was selected by a pyrolitic graphite monochromator. A 0.1-inch wide and 19-inch long collimation is applied to the incident beam to yield an achievable minimal q value of 0.025 Å^{-1}. The 32-wire detector simultaneously measures the scattered intensity at the scattering plane and swings (with respect to the sample) to 4 different positions to cover a q range from 0.025 to 0.25 Å^{-1}. The data were then corrected by the transmission, empty cell and background scattering. However, due to the smearing effect contributed by the vertical divergence, we are not able to compare the E3 data directly with the NG3 data. The measurements mainly provide a qualitative comparison among the samples.

3. Data analysis and results

The scattering data of the samples containing various ions (i.e., Cu^{2+}, Ni^{2+}, Zn^{2+}, separately and all together) obtained from E3 diffractometer (Fig. 2) indicate that the scattering pattern strongly depends on the pH values of the systems instead of the presence of the ions. All the curves of the samples in the basic condition collapse onto one curve with a low-q plateau followed by a high-q decay, indicative of small particles. This is different from all the scattering curves of the acidic samples, which have a common pattern that two monotonic decays with different slopes at low- and high-q regimes are observed. Due to a strong smearing effect from vertical divergence, a detailed analysis is not performed on these data. Instead, we analyzed the SANS data of the representative samples (S#1–S#4) obtained from NG3 30-m SANS instrument, which has a higher resolution.

The SANS data in Fig. 3 shows that S#1 and S#4 have a similar pattern, while S#2 and S#3 are almost identical to each other. This result confirms the E3 neutron diffraction data, indicating that pH value is one of the most influential parameters on morphology. The scattering intensity of S#1 at the low-q regime (from 0.003 to 0.05 Å^{-1}) follows a q^{-2} decay, a characteristic of scattering from two-dimensional objects, pre-

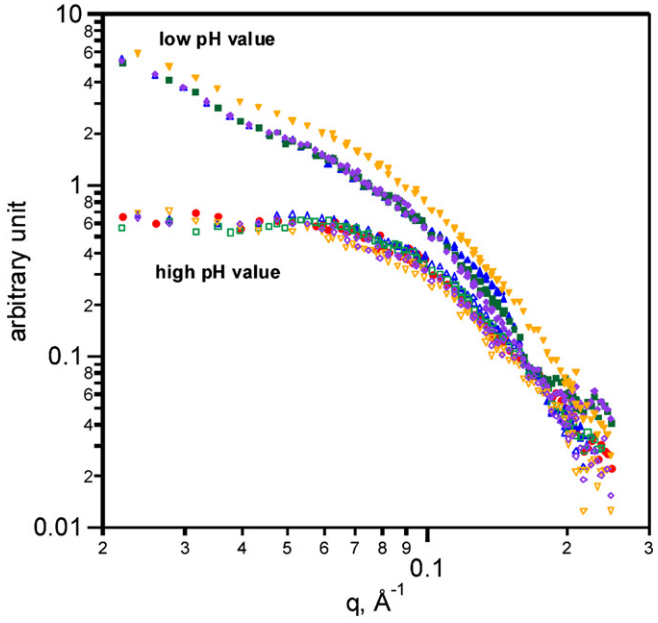

Fig. 2. CNBC E3 neutron diffraction data for samples of various ion dopants (no dopant: purple diamonds; Cu^{2+}: blue tip-up triangles; Ni^{2+}: green squares; Zn^{2+}: orange tip-down triangles; all ions [Cu^{2+}, Ni^{2+}, Zn^{2+}]: red circles) under acidic (solid symbols) and basic (open symbols) conditions.

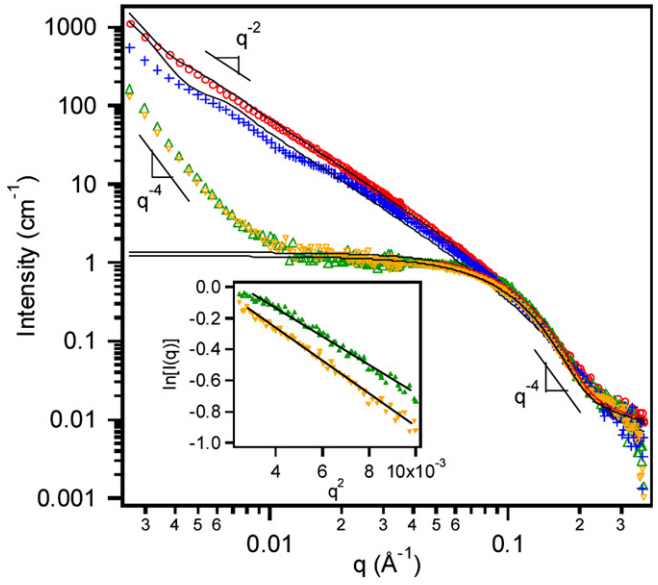

Fig. 3. NIST SANS data (represented by symbols) of S#1 (blue), S#2 (orange), S#3 (green) and S#4 (red). The solid curves are the best fitting results for S#1 and S#4 using the polydisperse spherical shell model and S#2 and S#3 using spherical model. The inset illustrates the Guinier plots [$\ln(I)$ vs q^2] of S#2 (orange) and S#3 (green). The slopes of the solid regression lines reveal the size of micelles ($=-R_G^2/3$).

sumably, unilamellar vesicles. Moreover, there are weak oscillations along the curve indicating the vesicular size distribution is somewhat narrow. Therefore, a simple model could be used, a polydisperse spherical shell [15], to fit the experimental data. The shell, presumably, is composed of the rhamnolipid bilayer and the best fitting result indicates a bilayer thickness of 15 ± 2 Å, an average diameter of 550 ± 50 Å and polydispersity of 0.28 ± 0.05.

The best fitting curve does not agree with the SANS data very well at low q, presumably due to the strong influence of interparticle interaction (known as the "structure factor") or the existence of another population of smaller aggregates (e.g., micelles). However, the feature of oscillation and the position of the broad peak are captured, indicative of reasonably reliable size and polydispersity from the best fitting result. In the case of S#4, whose pH value is lower than that of S#1, the scattering pattern also shows a q^{-2} dependence at low q. However, the absolute intensity is slightly higher than that of S#1 at the same q range and the intensity oscillation is almost absent with the broad peak seemingly shifting to a lower q value, indicative of a higher polydispersity and slightly larger particles in the system. After fitting the data using the same model, the bilayer thickness, diameter and polydispersity of the S#4 vesicles are obtained to be 14 ± 1, 580 ± 50, and 0.38 ± 0.10 Å, respectively.

For both S#2 and S#3 (under a strong basic condition), the intensity decays as a function of q^{-4} (corresponding to Porod's law [16] of scattering from the interface) at the low-q regime ($q < 0.007$ Å^{-1}), indicative of the existence of large aggregates (>200 nm). Then, the intensity remains practically constant over the q range between 0.012 and 0.06 Å^{-1} followed by another q^{-4} decay at $q > 0.1$ Å^{-1}, indicative of another population of smaller aggregates, possibly micelles (Fig. 2). The scattering intensity contributed from the micelles can be approximated as the following, where $R_G^2 q^2/3 \leqslant 1$:

$$I(q) \approx I(0) e^{-R_G^2 q^2/3}. \tag{1}$$

Here $I(0)$ and R_G is the zero-angle intensity and radius of gyration of the micelles [16]. A Guinier plot, where $\ln[I(q)]$ is plotted against q^2, can therefore be constructed to obtain the dimension of the micelles (inset of Fig. 3). This approach is based on the following two assumptions: the inter-micellar interaction is minimal, and the contribution of SANS intensity from large aggregates at the q region in interest (in this case, $q > 0.03$ Å^{-1}) is negligible. According to Eq. (1), the obtained slope of the line, $\ln[I(q)]$ vs q^2, is $-R_G^2/3$. Applying the Guinier plot on the SANS data over a q range between 0.04 and 0.1 Å^{-1} results in a value of $R_G = 17.2 \pm 1.0$ Å. The same data analysis can be applied to the scattering curve of S#3 as well. The obtained R_G is 17.9 ± 1.0 Å, which is practically the same dimension as that of S#2 within the error. Therefore, it can be concluded that they presumably have the same micellar structure. The data were also fitted by a spherical model (the solid curves) [17] yielding a radius of 17.5 Å for both cases confirming the result from Guinier analysis. Since the larger aggregates (causing the uprising at low q) are outside the scale of the SANS probing range, we cannot conclude the structure based on current SANS data. However, they are possibly not of unilamellar structure, since the scattering decay follows q^{-4} instead of q^{-2}.

4. Discussion

Previously, Andrä et al. [18] published the structure of R2 using small angle X-ray scattering and two structures of multilamellae and cubic phases were observed depending on the

concentrations and temperatures. Helvaci et al. [13] also reported a transition from lamellar to hexagonal phase in R1 and R2 solutions upon increased salt (NaCl) concentration based on the optical microscopic data. However, these experiments were conducted with relatively high lipid concentrations (>5%), while none of the above mentioned structures are found in our systems possibly due to the low concentration. Moreover, as mentioned previously, the morphology of the aggregates in the solution is strongly dependent on the pH of the system. In the case of adding 1% NaOH, a basic condition, the mixture forms large aggregates (>200 nm) + micelles whose R_G is ∼17 Å, while in the sample with 1% NaCl, in an acidic environment (pH 5.5), the mixture forms large polydisperse vesicles with a radius ∼600 Å, consistent with the early cryo-TEM results by Ishigami, et al. [19] and Champion et al. [12]. However, they did not observe the large aggregates under basic conditions, while SANS presents all the aggregates in the solutions. Another observation of the increased size of the vesicles with increased acidity, however is consistent with their result. This morphological transformation from large vesicles → small vesicles → micelles (coexisting with large aggregates) upon increasing pH value is presumably due to the increased charge density on the carboxyl group, resulting in a more repulsive hydrophilic head group and an increased effective size of the head group, thus intriguing the formation of high-curvature micelles [20]. The wall thickness of the vesicles (∼15 Å) seems thinner than that of normal phospholipid vesicles possibly due to a shorter hydrocarbon chain (only 7 carbons) but this is not totally unexpected. A detailed SANS study on the structure of a 6-carbon phospholipid (dihexanoyl phosphatidylcholine) solution shows that the lipid forms prolate micelles with a shorter axis of 17.8 Å, which is comparable to our best-fit result [21].

The neutron diffraction result indicates that the influence of metal ions on the morphologies is minimal in contrast to the study of Champion et al. [12] who found that the presence of cadmium decreased the vesicular diameter, because Cd^{2+} stabilized the vesicle structure. According to the findings of this study, one can also conclude that the size of aggregates in both acidic and basic conditions is fine enough to ease the flow of the rhamnolipid solution through the porous media with the pore sizes as small as 200 nm.

5. Conclusions

The global structures of R1 and R2 aggregates in solutions were successfully obtained using SANS and the result confirms the morphological transition reported with cryo-TEM data. Based on SANS data, it can also be concluded that pH is the determining factor for the transition. In fact, the pH-sensitive vesicles have the potential for the use of controlled release nanoparticles to deliver drugs. From an environmental standing point, the pH in the media to which the metal techniques applied is a major controlling parameter in the efficiency of the process. This is due to changes in the morphological transition of the rhamnolipid structure.

Acknowledgments

This work utilized facilities supported in part by the National Science Foundation under Agreement No. DMR-9986442. The authors would also like to acknowledge the financial support from NSERC, FQRNT, and Concordia University for the research and the supply of the rhamnolipid from Jeneil Biosurfactant Co.

References

[1] K. Hitsatsuka, T. Nakahara, N. Sano, K. Yamada, Agric. Biol. Chem. (1971) 686.
[2] K. Tsujii, Surface Activity, Principals, Phenomena, and Applications, Academic Press, San Diego, 1998.
[3] C.N. Mulligan, R.N. Yong, B.F. Gibbs, J. Hazard. Mater. 85 (2001) 111.
[4] C.N. Mulligan, B. Dahrazma, ASTM STP 1442 (2003) 208.
[5] S. Kyung-Hee, K. Kyoung-Woong, Environ. Geochem. Health 26 (2004) 5.
[6] C.N. Mulligan, R.N. Yong, B.F. Gibbs, Environ. Progr. 18 (1999) 50.
[7] J.E. McCray, G. Bai, R.M. Maier, M.L. Brusseau, J. Contam. Hydrol. 48 (2001) 48.
[8] B. Dahrazma, C.N. Mulligan, Prac. Period. Hazard. Toxic Rad. Waste Manag. 8 (2004) 166.
[9] C.N. Mulligan, B. Dahrazma, in: 15th International Biohydrometallurgy Symposium (IBS), Athens, 2003.
[10] B. Dahrazma, C.N. Mulligan, J. ASTM Int. 3 (2006) 7.
[11] Y. Zhang, R.M. Miller, Appl. Environ. Microbiol. 58 (1992) 3276.
[12] J.T. Champion, J.C. Gilkey, H. Lamparski, J. Retterer, R.M. Miller, J. Colloid Interface Sci. 70 (1995) 569.
[13] S.S. Helvaci, S. Peker, G. Özdemir, Colloids Surf. B 35 (2004) 225.
[14] C.J. Glinka, J.G. Barker, B. Hammouda, S. Krueger, J.J. Moyer, W.J. Orts, J. Appl. Crystallogr. 31 (1998) 430.
[15] M.-P. Nieh, C.J. Glinka, S. Krueger, R.S. Prosser, J. Katsaras, Biophys. J. 82 (2002) 2487.
[16] G. Porod, in: O. Glatter, O. Kratky (Eds.), Small Angle X-Ray Scattering, Academic Press, New York, 1982, chap. 2.
[17] S.R. Kline, J. Appl. Crystallogr. 39 (2006) 895.
[18] J. Andrä, J. Rademann, J. Howe, M.H.J. Koch, H. Heine, U. Zähringer, K. Brandenburg, Biol. Chem. 387 (2006) 301.
[19] Y. Ishigami, Y. Gama, H. Nagahora, J. Am. Oil Chem. Soc. 64 (1987) 1265.
[20] Y. Ishigami, S. Suzuki, Prog. Org. Coat. 31 (1997) 51.
[21] T.-L. Lin, S.-H. Chen, N.E. Gabriel, M.F. Roberts, J. Am. Chem. Soc. 108 (1986) 3499.